

Development and characterization of *in situ* gelling system containing atorvastatin-loaded polycaprolactone nanoparticles for periodontal diseases

Sedat ÜNAL^{1*} , Osman DOĞAN² , Heybet Kerem POLAT³ , Yeşim AKTAŞ¹ 

¹ Department of Pharmaceutical Technology, Faculty of Pharmacy, Erciyes University, Kayseri, Türkiye

² Department of Pharmaceutical Technology, Faculty of Pharmacy, Hacettepe University, Ankara, Türkiye

³ Republic of Türkiye Ministry of Health, Turkish Medicines and Medical Devices Agency, Ankara, Türkiye

* Corresponding Author. E-mail: sedatunal@erciyes.edu.tr (S.Ü); Tel. +00-000-000 00 00.

Received: 10 April 2023 / Revised: 05 May 2023 / Accepted: 05 May 2023

ABSTRACT: The periodontal pocket provides a suitable environment for bacterial accumulation and growth which results in ultimately tooth loss. The clinical efficacy of current therapy for periodontal pocket is low because the flushing actions within the mouth causes to rapid clearance of the solution. The antioxidant and anti-inflammatory effects of atorvastatin (ATV) can facilitate healing process of periodontal diseases. The aim of this study was to develop *in situ* gel formulation containing ATV-loaded polycaprolactone nanoparticles (PCL-NPs). PCL NPs were prepared by nanoprecipitation method. The NPs had spherical shape with a particle size range of 176-329 nm. They showed 59% encapsulation efficiency and prolonged release profile. In order to increase the mucoadhesive properties of the formulation and the residence time of the drug at the site of action, NPs were incorporated to *in situ* gel to provide a combination therapy. *In situ* gel formulation was prepared by cold method and characterized in terms of pH, gelation temperature and time, viscosity, syringeability, and rheological behaviours. *In vitro* release studies revealed that *in situ* gel formulation remarkably extend the release time of ATV and mathematical release kinetic modelling shows formulations can fit multiple models. The overall findings indicated that the combination therapy strategy of locally administration of *in situ* gel containing ATV-loaded polycaprolactone nanoparticles to periodontal pockets is a promising and innovative approach.

KEYWORDS: Polycaprolactone; atorvastatin; nanoparticles; periodontal diseases; *in situ* gel; combination therapy

1. INTRODUCTION

Periodontium is a unique interface, between teeth and their supporting tissues in terms of anatomical structure. It has three main functions (i) supporting the tooth; (ii) preventing tooth from oral microflora; (iii) enabling the attachment of the tooth to the bone [1]. Periodontal pocket offers a convenient environment for growth of pathogenic bacteria that might trigger inflammatory response. Periodontitis refers to inflammation process in periodontium initiated by bacterial infection or trauma that leads to destruction of surrounding periodontal tissue, which is called periodontal pocket, and eventually the tooth [2]. Although the underlying mechanisms of periodontitis are not thoroughly understood, two reasons are well established; bacterial infection and inflammatory responses [3]. Immune response at normal level is likely to induce proteolytic cleavage, synthesize of pro-inflammatory cytokine while abnormal immune response may cause a number of diseases such as autoimmune, metabolic diseases [4]. Therefore, most novel therapeutic approaches regarding periodontitis focus on host inflammation response modulation.

Originally statins have been used for patients with cardiovascular diseases in order to decrease cholesterol level by inhibiting 3-hydroxyl-3-methylglutaryl coenzyme A (HMG-CoA) reductase which is a key component in cholesterol synthesis [5]. Recent numerous studies have pointed out that in addition to anti hypercholesterolemic effect, statins exhibit protective effects by decreasing the secretion of pro-inflammatory cytokines and inhibit the production of chemokine from macrophages [6,7,8]. Atorvastatin

How to cite this article: Ünal S, Doğan O, Polat HK, Aktaş Y. Development and characterization of *in situ* gelling system containing atorvastatin-loaded polycaprolactone nanoparticles for periodontal diseases. J Res Pharm. 2023; 27(5): 1951-1973.

(ATV) belonging to the statin group is a commonly prescribed medicine. However, ATV has poor oral bioavailability (12%) because of extensive first pass effect [9]. Thus, high-dose ATV needs to be used in treatments resulting in liver damage. In addition to that, ATV is a quite lipophilic molecule so that it has low aqueous solubility [10]. To overcome these problems, novel delivery systems can be a promising strategy.

Traditional therapeutic agents suffer from various problems such as poor solubility of molecules, extent first pass effect, high and frequent doses to reach required therapeutic index, systemic severe adverse effect and toxicity. The use of nanotechnological approaches is increasingly becoming important to circumvent these barriers. Particularly, in recent years, polymeric nanoparticles (NPs) have received great deal of attention. Polymeric NPs increase the drug stability by protecting it from degradation in biological environment and provide controlled drug release profile [11]. They play essential role in the use of lipophilic molecules in treatment. Polymeric NPs either entrap the molecules within core or carry the drug on their surface [12]. Thus, aqueous solubility of lipophilic compounds is improved. Polycaprolactone (PCL) is one of the most preferred biocompatible and biodegradable polymers in clinical studies owing to non-toxicity, its permeability features and slow degradation rate [13,14,15,16].

Surface coating technology has become an indispensable part of improving NP formulations. Several surface modification materials have been used to increase solubility and permeability; chitosan (CS) polymer is one of them. CS is deacetylated form of chitin and naturally derived from the exoskeletons of insects [17]. Since CS is a non-toxic and biocompatible, it has been widely utilized in drug delivery systems, DNA & RNA carrier, and surface coating [18]. Furthermore, another issue worthy of consideration relates to the main problem of majority of drugs is that due to the mucoadhesive character of CS, molecules coated with CS accumulates more in mucosa [19].

A continuous flow of crevicular fluid occurs in the complex area of the periodontal pocket, where local drug distribution is intended to take place. An injectable *in situ* sustained release gel would be a suitable solution to achieve the therapeutic effects of the drug in the challenging environment. A cutting-edge technique now being employed to achieve this goal is *in situ* gel-forming formulations. These formulations are in liquid phase during application but form strong gels at the delivery site [20]. Among *in situ* gelling polymers, thermosensitive systems like poloxamer stand out to be used in injection into periodontal pockets. Poloxamer exhibits amphiphilic behaviour because of the hydrophilic ethylene oxide region and the hydrophobic propylene oxide region. Ability of poloxamer may be explained by the differences in micellar structure that depends on temperature and concentration change. The main disadvantage of poloxamer is its lacking mucoadhesive property. Therefore, additional polymers, such as chitosan, carbopol, and hydroxypropyl methyl cellulose (HPMC), have been used to enhance the mucoadhesive characteristics of ocular formulations based on poloxamer [21,22].

In the current study, firstly, ATV loaded PCL nanoparticles were prepared by nanoprecipitation method. NPs were coated with CS to enhance mucoadhesive character of PCL NPs. Recent studies pointed out that polymer concentration remarkably influences characteristics of NPs including encapsulation efficiency, particle size, release profile [23,24,25]. Thus, two different concentrations of PCL were used in this study, 0.5% and 0.25%. Then, NPs were characterized by polydispersity index, particle size, zeta potential. Drug encapsulation efficiency was determined by UV spectrophotometry. *In vitro* ATV release from PCL NP was tested to calculate the potential of PCL nanoparticulate system. Later, ATV-loaded NPs were included into *in situ* gel formulations, which were produced to extend the residence period of the nanoparticles on the periodontal pocket. These formulations included the thermosensitive polymer poloxamer 407 (PL 407) as well as the mucoadhesive polymer HPMC. The optimum formulation was chosen, the release research was conducted using that formulation, and *in vitro* characterization experiments of the produced *in situ* gels were performed.

2. RESULTS AND DISCUSSION

2.1. Characterization of Prepared Nanoparticles

2.1.1. Determination of particle size, PDI and surface charge

The mean particle size is mainly related to tissue targeting, clearance of drug from blood, interaction with cell surface, cellular uptake. NPs with larger diameter can be detected easily by the mononuclear phagocytic system cells [26]. On the other hand, small NPs are removed by renal excretion and might cause several toxic effects due to greater surface area [27,28]. Thus, NPs size should be strictly controlled in optimum range to prevent adverse effects and capillaries' occlusion. As shown in Figure 1, in this study NPs ranged from 176 ± 1.0 nm to 227 ± 2.4 nm for 0.25% PCL concentration and from 212 ± 1.6 to 329 ± 4.6 for 0.5% PCL concentration with acceptable range for medical applications. As shown in Table 1, there is a noteworthy positive correlation between PCL concentration and particle size. Our findings exert similarity to results reported by Chorny et al. and Tavares et al. [29,24]. Increasing PCL concentration brings more viscous organic phase resulting in larger and intense nanodroplets formation in the aqueous phase. The same effect was reported by Miladi et al. [30].

PDI is a parameter used to portray homogeneity ratio of formulations. Formulations exhibiting high homogeneity in particle size are described as monodisperse system. PDI values below 0.4 are considered suitable. As illustrated in Table 1, PDI values were in the range of 0.09-0.245. Results pointed out that the PCL NPs had a monodisperse formation, but increase in PCL concentration led to higher PDI values. Similar study conducted by Roldan et al. reported that enhancement of polymer concentration increases the PDI values [31].

Surface charge has crucial role particularly in cellular uptake, biodistribution of NPs. Cellular membranes and mucosa have negatively charged surfaces. Thus, cationic particles have a tendency to accumulate in cellular membrane and mucosa [32]. On the other hand, high surface charge prevents NPs from aggregation because of strong electrostatic repulsive among the NPs [33]. Particles with zeta potentials more positive than +30 mV or more negative than -30 mV are normally considered stable. Since PCL NPs are negatively charged because of the terminal carboxylic group, cationic CS was used as the coating material to enhance the cellular uptake of the NPs. As shown in Table 1, uncoated NPs had low and negative charge, while surface charge of CS coated NPs both increased and changed positively. Positive charge of CS arises from its high-molecular weight heteropolysaccharide structure [34].

Table 1. Mean particle size, PDI and zeta potential of blank and ATV-loaded PCL nanoparticles prepared with different concentration of polymer (Organic solvent is acetone, CS concentration is 0.025 % (w/v), Pluronic F-68 concentration is 0.75% (w/v), organic phase:aqueous phase ratio 1:2 (v:v)) (n= 3, ± SD).

PCL-NP Formulations			Particle Diameter ± SD (nm)	PDI ± SD	ZP ± SD (mV)
PCL% (w/v)	Formulation Code	Blank/PCX loaded			
0.25	PCL NPs	Blank	176.0±1.1	0.090±0.004	-20.1±1.6
		ATV loaded	188.0±1.8	0.113±0.012	-22.7±1.9
	CS/PCL NPs	Blank	206.0±1.9	0.133±0.014	+38.8±3.3
		ATV loaded	227.0±2.4	0.146±0.041	+37.3±5.9
0.5	PCL NPs	Blank	212.0±1.6	0.128±0.013	-25.4±2.1
		ATV loaded	228.0±2.3	0.155±0.011	-28.1±3.2
	CS/PCL NPs	Blank	301.0±3.7	0.211±0.018	+33.4±3.9
		ATV loaded	329.0±4.6	0.245±0.026	+31.6±4.4

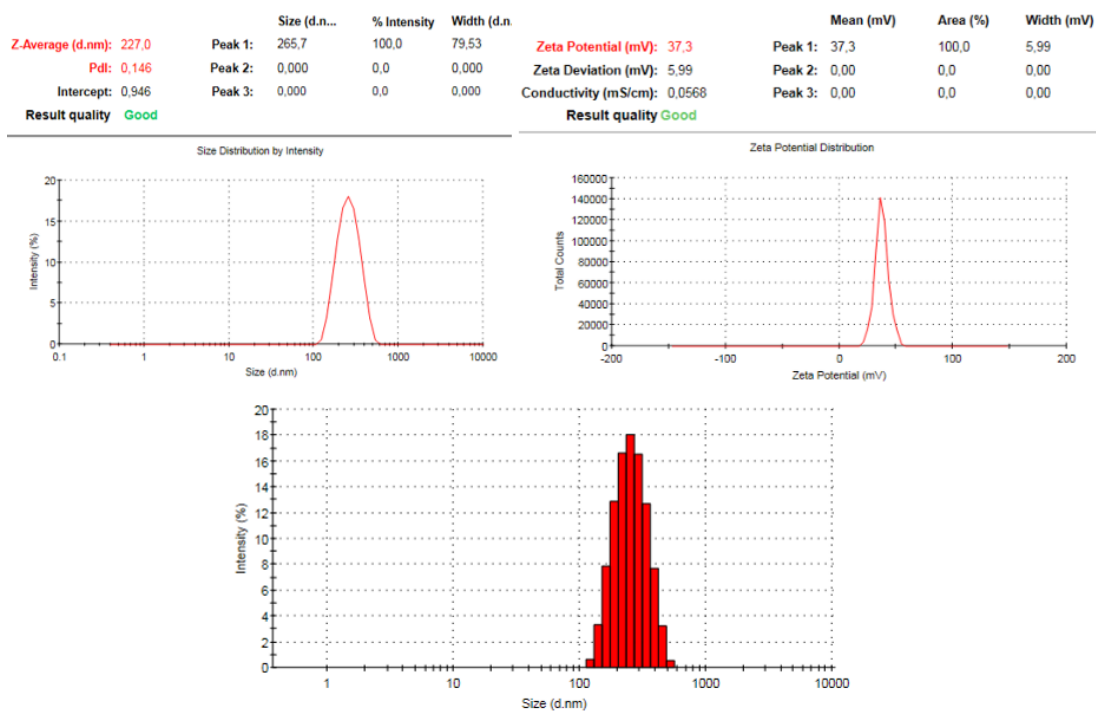


Figure 1. Analysis results of nanoparticles by Malvern Zetasizer Nano ZS. Representative images are presented for ATV-loaded CS coated PCL NPs (CS/ATV-PCL NPs) (0.25% (w/v) PCL).

2.1.2. Determination of entrapment efficiency

Table 2 illustrates the percentages of encapsulation efficiency and drug loading of PCL NPs prepared with different polymer concentrations. Formulation with 0.25% w/v PCL exhibited 37.6%-49.4% and 3.9%-5.4% encapsulation efficiency and drug loading, respectively. Encapsulation efficiency and drug loading of NPs prepared with 0.5% w/v PCL ranged 44.2%-59.1% and 4.7%-6.9% respectively.

It is observed that the increase in polymer concentration considerably increased the encapsulation efficiency and drug loading of formulations. The increase in polymer concentration results in firmer and more viscose organic phase which forms bigger particles in the aqueous phase [35]. In addition to that, CS used as coating material led to increase in entrapment efficiency as coating materials provide more drug molecules adsorbed onto the surface of the NPs [36]. As shown in our results, CS remarkably enhanced the encapsulation efficiency and drug loading of formulations.

Table 2. The percentages of encapsulation efficiency and drug loading of ATV-loaded PCL nanoparticles prepared with different polymer concentrations.

PCL-NP Formulations		Encapsulation efficiency % \pm SD (EE)	Drug loading % \pm SD(DL)
PCL% (w/v)	Formulation Code		
0.25	ATV-PCL NPs	37.6 \pm 1.3	3.9 \pm 0.2
	CS/ATV-PCL NPs	49.4 \pm 1.9	5.4 \pm 0.6
0.5	ATV-PCL NPs	44.2 \pm 1.6	4.7 \pm 0.4
	CS/ATV-PCL NPs	59.1 \pm 2.1	6.9 \pm 0.7

2.1.3. Nanoparticle Morphology Characterization

In order to investigate the morphological characterization of PCL NPs, formulations were analysed by SEM. As illustrated in Figure 2, the shape of PCL nanoparticles was smooth and spherical. NP size varied between 190-337 nm which are consistent with results measured by DLS. As shown in SEM pictures, the increase in polymer concentration and coating increased the size of NPs.

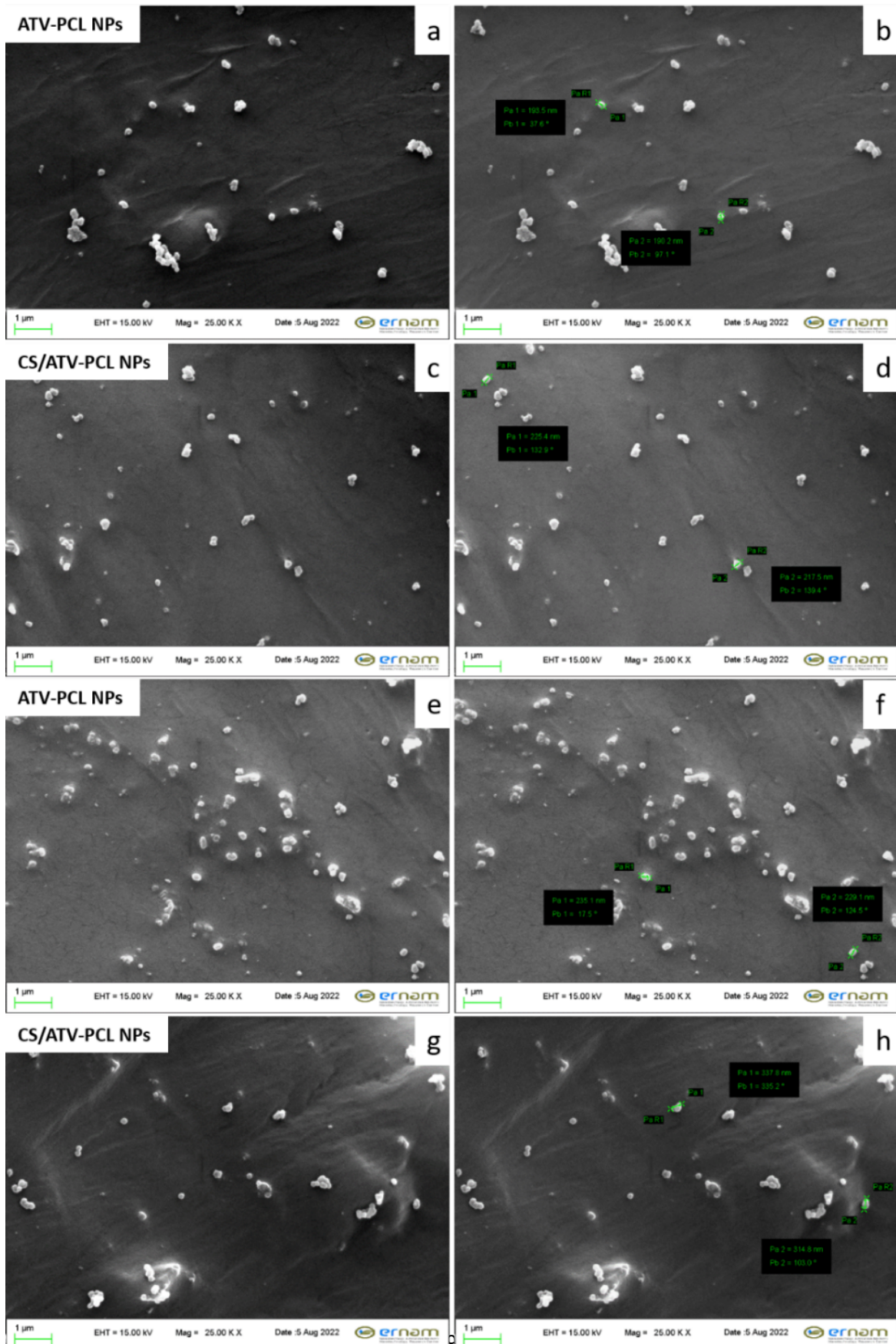


Figure 1. Scanning electron microscopy (SEM) micrographs of ATV-loaded NPs. (a,b) ATV-PCL NPs. (c,d) CS/ ATV-PCL NPs. (a,b,c,d; PCL concentration 0.25% (w/v)). (e,f) ATV-PCL NPs. (g,h) CS/ ATV-PCL NPs. (e,f,g,h; PCL concentration 0.5% (w/v)). (b,d,f,h; Representative images with measuring scales)

2.1.4. *In vitro* release of ATV from PCL nanoparticles

In vitro release studies of optimized NPs were performed to get an insight into the release behaviour, release mechanism and kinetics. Figure 3 summarizes the *in vitro* release profile of ATV from PCL NPs. As it can be seen in release graphic, in the study, a biphasic release profile was reported, the first burst release was observed in the first 4 hours, followed by a sustained release profile. It is clearly seen that NPs prepared with high concentration PCL had slower release for both coated and uncoated groups. High concentration polymer leads to increase of viscosity in organic phase which hampers the diffusion of organic phase into aqueous phase. As a result, bigger NPs are formed. In the literature, there are studies previously reported which confirm that larger NPs extend the release time of drug from NPs [30].

CS coating significantly prolonged the release time. CS is a cationic polysaccharide which shows strong interaction with negatively charged compounds. Therefore, CS on the NPs surface establishes vigorous interaction with anionic ATV and provides sustained release profile [37]. Similarly, in our study, CS-coated formulations provided the prolonged release time. Within the scope of the burst effect, CS coating led to more adsorption of the ATV molecules on the NPs surface. Therefore, drug molecules attached to surface of the NPs rapidly liberate from the NPs. Similarly, Nagarwal et al. reported results which are in accordance with our results [38]. According to study conducted by Nagarwal, they observed that CS coating significantly increase drug loading capacity from 2.68% to 18.93%.

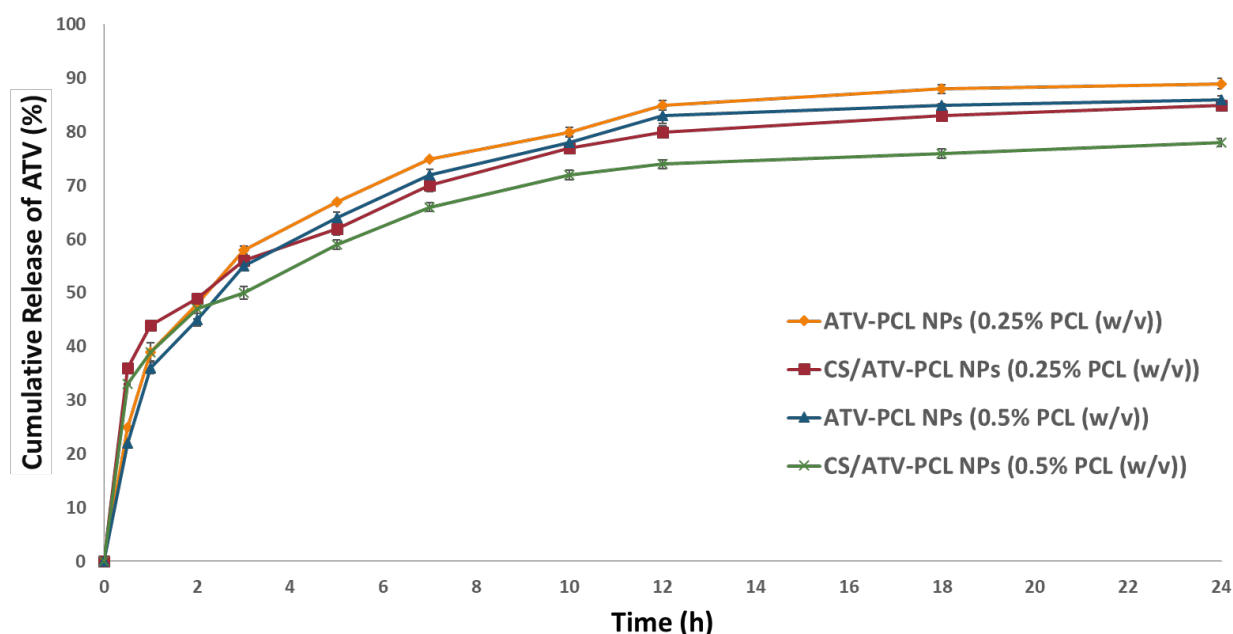


Figure 3. *In vitro* release profiles of formulations (n=3)

2.2. *In situ* Gel Preparation and Evaluation

2.2.1. Characterization of *in situ* gel formulations

The *in vitro* characterization results belonging to *in situ* gel formulations are illustrated in Table 4. The gelation times for all *in situ* gel formulations were found to be between 24±0.5 and 51±0.8 s. The gelation temperature for all *in situ* gel formulations were found to be between 40±0.7 and 24±0.8°C. The pH of all formulations ranged between 7.08±0.03 and 7.12±0.01. According to studies, it can be syringed using a 20 gauge needle.

As a result, for all formulations, viscosity was determined at 10 rpm at both 25°C and 37°C. The results showed that viscosity values vary depending on the quantity of polymer (Table 3).

Table 3: Results of *in situ* gels' *in vitro* characterization analysis

Formulation	pH (±SD)	Gelation temperature (°C±SD)	Gelation time (s)	Viscosity (cP) 25°C	Viscosity (cP) 37°C
TB1	7.12±0.01	40.0±0.7	51.0±0.8	251±26	552±81
TB2	7.09±0.02	35.0±0.4	39.0±0.4	283±23	9852±136
TB3	7.08±0.01	29.0±0.9	32.0±0.5	587±54	14568±194
TB4	7.08±0.03	24.0±0.5	25.0±0.7	9263±247	17141±282

All formulations have pH values between 7.08±0.03 and 7.12±0.01. The pH values fall within this range because of the nature of the polymer [39]. The formulation will be buffered in biological environment by raising the pH of the solution to 7.4 [41].

For oral application, 19-27 gauge hypodermic syringe are used [41]. Syringeability test was performed to provide that the formulations have proper flowability to bind to the mucosal surface. According to the syringeability examination with a 20-gauge hypodermic needle-syringe system, all formulations were found to be syringeable. These needles are said to support deeper skin, bone, or tooth penetration and allow for more viscous drugs.

An ideal thermosensitive dental system should have a greater sol-gel transition temperature ($T_{sol/gel}$) than room temperature, preferably 30°C, and form a gel at dental temperature (37°C), despite of being diluted in the mouth cavity [21]. It was noted that the gelation temperature reduced from 40±0.7°C to 24±0.5°C while the concentration of PL 407 increased from 15% (TB1) to 24% (TB2). PL 407 is an ABA-type triblock copolymer (PPO-PEO-PPO) that consists of a hydrophobic polypropylene oxide (PPO) and hydrophilic polyethylene oxide (PEO) units. Amphiphilic block copolymer molecules can form tiny micellar subunits in aqueous liquids. The critical micelle concentration is the point at which the polymer molecules assemble to create a vast, cross-linked network of micellar molecules [42]. Temperature is also a major determinant in micelle production. Propylene oxide (PO) is relatively soluble in aqueous solutions and both the ethylene oxide (EO), and PO blocks are hydrated at temperatures below the critical micelle temperature. Increase in temperature leads to hydrophobic interactions between PPO units, dehydration, and less solubility than the PEO chains. This causes the creation of spherical micelles,

which have a dehydrated PPO core and an outer tumid hydrous PEO shell. It can be challenging for micelles to disperse independently in the solution and instead interact and tangle with other micelles resulting in a three-dimensional network structure [43]. As a result, gelation requires a greater temperature at lower PL 407 concentrations. However, it is believed that the use of HPMC has caused the lower gelation temperatures. El-Enin and Gina previously reported on HPMC's ability to lower gelling temperatures while evaluating tenoxicam liquid suppository [44]. This could be explained by capacity of HPMC to form hydrogen bonds with the POE chains found in PL 407 molecules, which encourages dehydration and increases the entanglement of nearby molecules, producing gelation at lower temperatures [45].

Ideally, it is expected that the system gels instantly or within a brief time when temperature of system reaches its gelation temperature. Therefore, quick removal of formulation by tear periodontal pocket is prevented to some extent. It was recorded that all formulations exhibited a quick gelation time of about between 25 and 51 s (Table 3). It is also noticed that ATV containing higher PL407 concentration exerted shorter gelation time compared to other formulations. This consequence points out that, the decrease of effective sol-gel transition temperature related with higher poloxamer concentration, is accompanied by shorter gelation time [46].

In order to assess the viscosity of the formulations prior to gelling at 25°C, and at the physiological temperature of 37°C, rheological evaluations of all *in situ* gelling systems were conducted. When working with concentrated or complex formulations incorporating high molecular weight polymers like PLA, and HPMC, syringeability and injectability are two crucial considerations [47]. Additionally, tests were done to assess the rheological characteristics of *in situ* gels at various rpm, and it was found that all *in situ* gels exhibited pseudoplastic flow (Figure 4).

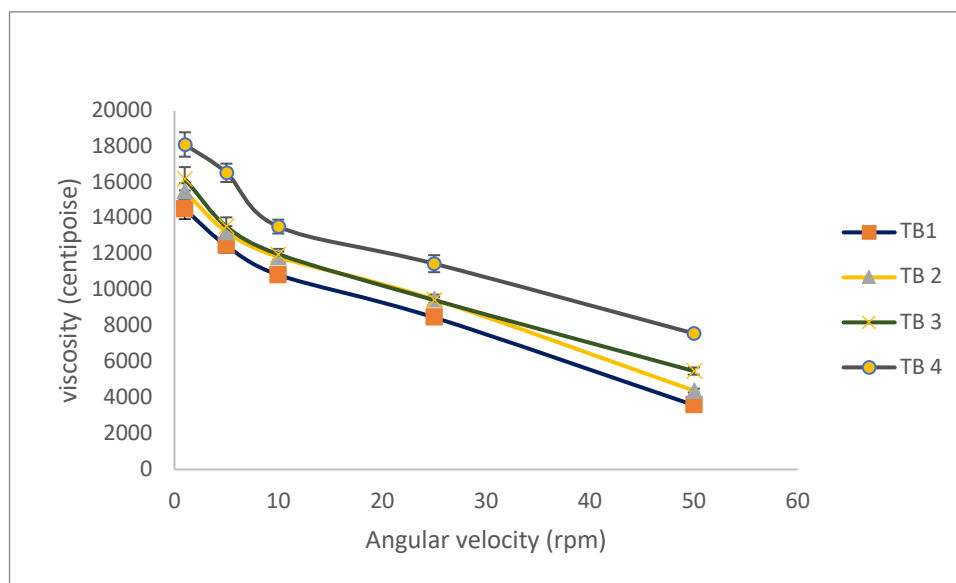


Figure 4. Rheological profiles of *in situ* gelling systems

For simple syringeability and injectability, an injectable *in situ* gel solution should have a viscosity of between 5-1000 centipoise and exhibit shear thinning property. Viscosity and shear rate are inversely proportional. The reduction in viscosity causes to increase the shear rate [48]. These two criteria must be met to guarantee that the formulations can be syringed and injected without significantly discomforting the patient.

Due to the relatively limited amount of gel that may be injected into periodontal pockets, it must be thickened for better retention and medication release management. The formulation, on the other hand, needs to have the right viscosity so that it may easily infuse in the periodontal pocket. As a result, for all formulations, viscosity was determined at 10 rpm at both 25°C and 37°C. The results showed that

viscosity values varied depending on the quantity of polymer (Table 2). This example demonstrates how the concentration of the polymer has a big impact on viscosity. The conclusions are consistent when the findings are examined in a literary context [49].

Results of all these characterization studies indicated that TB2 was the most suitable formulation for dental practice, and it was utilized for *in vitro* release studies. Regarding the NP formulation, since formulations prepared with 0.25% PCL concentration had lower PDI and particle size, they were preferred for *in vitro* release studies and determination of kinetic models TB2 *in situ* gel formulation was loaded with two different ATV-loaded NPs (ATV-PCL-NPs and CS/ATV-PCL-NPs). KRH is ATV-PCL embedded *in situ* gel formulation and MRT is CS coated ATV-PCL embedded *in situ* gel formulation. In order to determine whether drug-loaded nanoparticles change the characterization of *in situ* gels, characterization was performed in drug-loaded *in situ* gels and the results are demonstrated in Table 4. The results revealed that there was no change in the gels with the drug loading.

Table 4. Physical properties of drug containing formulations and their component.

Formulation components and Physical Properties	KRH (ATV-PCL embedded <i>in situ</i> gel formulation)	MRT (CS/ATV-PCL embedded <i>in situ</i> gel formulation)
ATV-PCL NPs	0.5	0
CS/ATV-PCL NPs	0	0.5
PL407	15	15
HPMC 4KM	1	1
Distilled Water	100 mL	100 mL
pH (\pm SD)	7.09 \pm 0.01	7.08 \pm 0.01
Gelation temperature ($^{\circ}$ C \pm SD)	37.0 \pm 0.3	37.0 \pm 0.1
Viscosity (centipoise) 25 $^{\circ}$ C	264 \pm 35	271 \pm 39
Viscosity (centipoise) 37 $^{\circ}$ C	9645 \pm 317	9852 \pm 422
Gelation Time (s)	38.0 \pm 0.2	40.0 \pm 0.3

2.2.2. *In vitro* release

In vitro release studies of selected ATV-PCL NPs-loaded *in situ* gel formulations (KRH, MRT) were carried out in an isotonic phosphate buffer (pH 7.4) at 35 $^{\circ}$ C. As shown in Figure 5, release profiles revealed that there were noticeable variations between formulations.

Comparison of release profiles revealed a considerable difference between formulations (Figure 5). The overall release percentage for ATV loaded NPs was 89 \pm 0.8% and 85 \pm 1.01%. When MRT and KRH are examined, it is seen that drug release is between 82 \pm 0.7% and 75 \pm 0.8, respectively. Figure 6 indicates the cumulative release percent of ATV loaded NPs were 58 \pm 0.74% and 56 \pm 0.76%, respectively in the first three hours. When MRT and KRH were examined from 0h-3h, it is seen that drug release is between 49 \pm 0.9% and 51 \pm 1.2%. This indicates that *in situ* gel provided NP formulations with more sustained drug release than simple NPs due to the fact that drug molecules released from NPs entrapped into gel matrix. Similarly, Laddha et al. prepared pioglitazone-loaded PLGA nanoparticles in their study and loaded these nanoparticles in to a thermosensitive *in situ* gel they prepared with poloxamer. When *in vitro* release studies were examined, it was determined that it first made an burst release and then resulted in a controlled release [50]. Considering the coating material, CS/ATV-PCL NPs-loaded *in situ* gel significantly prolonged the release time. In the first 3 hours highlighted in Figure 6, it was observed

that ATV release from CS-coated formulations exhibited burst effect, followed by slow release. The initial burst release from the CS-coated NPs is because of adsorbed drug molecules on the shell of the NPs. CS coating significantly ($p < 0.05$) increased the amount of the adsorbed drug molecules on the shell of the NPs for both formulations. Our results are in accordance with those of a previously reported study [38].

In our prior erosion study, poloxamer gel degraded completely in 8 hours. It is plausible to believe that *in situ* gel release profiles were composed of the following two steps: In the first step, when the *in situ* gel slowly disintegrated, the NPs were concurrently released from the skeletal carrier. Slow release of the drug molecules from the PCL NPs was the second step. The disparities between the two release profiles of the two formulations were now explicable. At first, the gel prevented the ATV-loaded NPs from contacting the release medium. As the gel gradually deteriorated, a greater quantity of ATV is release from the NPs. Because the release behaviour of NPs was dependent on a diffusion mechanism, they all released at a rate that was comparable to that of atorvastatin-loaded NPs at 24 hours, after the gel had entirely dissolved. *In situ* gel formulation has clearly hindered the burst release and provided more sustained drug release profile. There are several studies similar to these results [21,46,51,53].

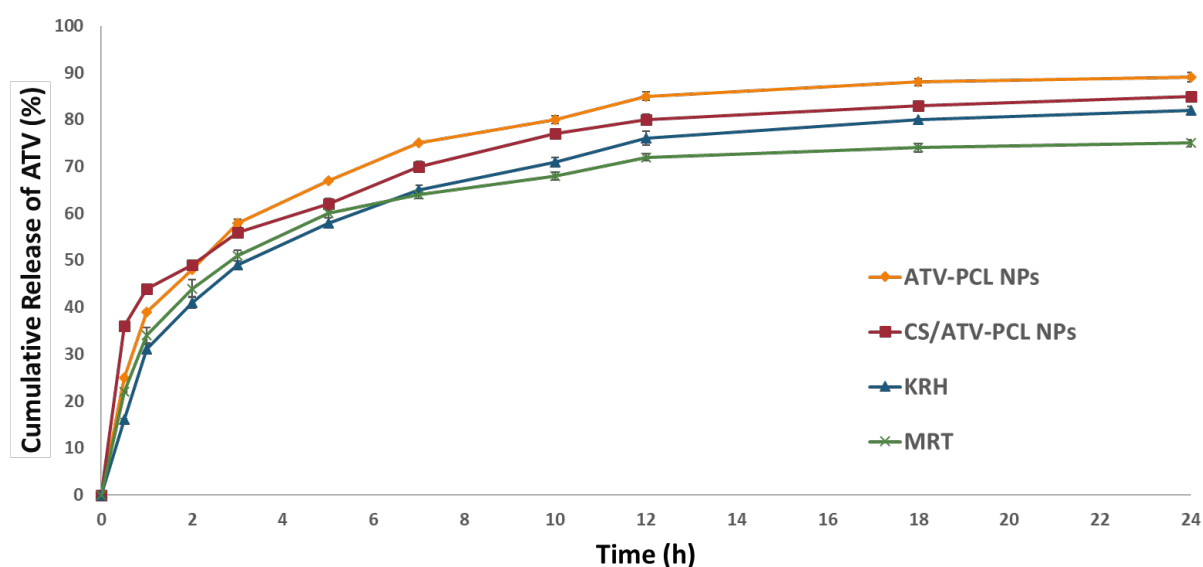


Figure 5. Cumulative release of ATV from NPs and *in situ* gel formulations containing ATV-loaded NPs (n=3)

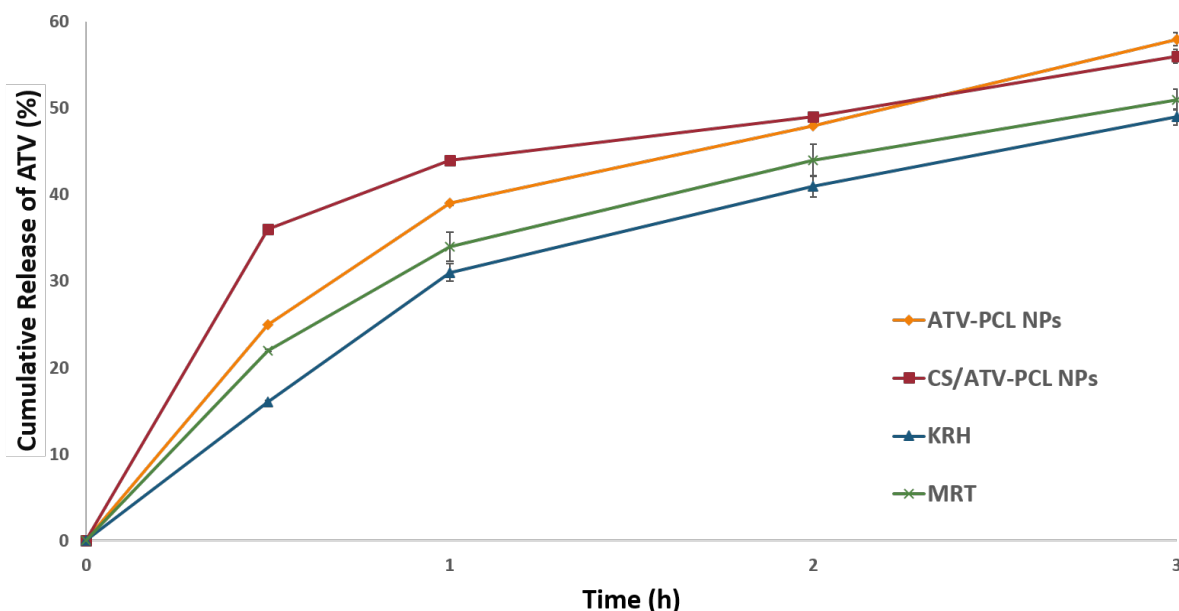


Figure 6. First 3 hours of the cumulative release of ATV from NPs and *in situ* gel formulations containing ATV-loaded NPs (n=3)

2.2.3. *In Vitro* Release Kinetic

Kinetic modeling parameter and graphics of ATV release from PCL NPs for both simple and *in situ* gel formulations are shown in Table 5 and Figure 7. According to the results, the formulations were found to fit to Peppas-Sahlin and Weibull model except for the CS-coated PCL NPs. For CS-coated PCL NPs, Peppas-Sahlin and Korsmeyer-Peppas models were found to be best fitted models. In the literature, there are several studies showing that one system can fit multiple models [53,54].

The *n* value is the diffusional exponent describing the drug-release mechanism, for Korsmeyer-Peppas model. If “*n*” value below 0.45, it means that release mechanism shows Fickian diffusion. If “*n*” value is between 0.45 and 0.85, the drug release occurs through a non-Fickian diffusion mechanism and if *n*=0.85 the transport occurs by swelling [55]. According to *n* value, CS/ATV-PCL NPs is compatible with Fickian diffusion. In the Weibull model, the “*β*” exponent is a parameter to explain the mechanism of release of drug through the polymeric NP matrix. While *β* below 0.75 indicates Fickian diffusion, *β* value between 0.75 and 1 indicates a combined mechanism of Fickian diffusion and swelling controlled release [56]. For the ATV-PCL NPs, KRH, and MRT, *β* value is 0.483, 0.517, and 0.401, respectively. The *β* values exhibit that these formulations complied with Fickian diffusion. “*m*” coefficient in Peppas-Sahlin model is equal to the coefficient “*n*” of Korsmeyer-Peppas [57]. In this context, “*m*” coefficient of all formulations was found to be equal to 0.45 or below 0.45. These results pointed out that ATV release from PCL NPs and *in situ* gel formulations was driven only by Fickian diffusion.

Comparison of each formulation is displayed in Table 6 in terms of similarity and difference factors. For all formulations, *f*₁ factors were <15 and *f*₂ factors were > 50. This confirmed that drug release profile of formulations exhibited similarity to each other.

Table 5. Release kinetic modeling and results of ATV-loaded PCL NPs

Model and equation / Formulation		Evaluation criteria						
		Parameter	R ²	R ² _{adjusted}	AIC	MSC	n/m*	
Zero-order F=k0*t	ATV-PCL NPs	k0	5.455	0.2663	-0.2663	103.9074	-0.9698	-
	CS/ATV-PCL NPs	k0	5.187	0.6648	-0.6648	104.1593	-1.4363	-
	KRH <i>in situ</i> gel	k0	4.904	0.0273	0.0273	99.6909	-0.6031	-
	MRT <i>in situ</i> gel	k0	4.634	0.4193	-0.4193	101.2946	-1.1267	-
First-order F=100*[1-Exp(-k1*t)]	ATV-PCL NPs	k1	0.182	0.8114	0.8114	82.9613	0.9344	-
	CS/ATV-PCL NPs	k1	0.157	0.5565	0.5565	89.6082	-0.1134	-
	KRH <i>in situ</i> gel	k1	0.140	0.8152	0.8152	81.4207	1.0578	-
	MRT <i>in situ</i> gel	k1	0.121	0.5609	0.5609	88.3898	0.0464	-
Higuchi F=kH*t^0.5	ATV-PCL NPs	kH	23.395	0.7523	0.7523	85.9614	0.6617	-
	CS/ATV-PCL NPs	kH	22.409	0.6105	0.6105	88.1812	0.0163	-
	KRH <i>in situ</i> gel	kH	20.797	0.8450	0.8450	79.4886	1.2334	-
	MRT <i>in situ</i> gel	kH	19.993	0.6923	0.6923	84.4784	0.4020	-
Korsmeyer-Peppas F=kKP*t^n	ATV-PCL NPs	kKP	37.139	0.9577	0.9530	68.5236	2.2469	0.321
	CS/ATV-PCL NPs	kKP	43.128	0.9907	0.9896	49.1523	3.5644	0.233
	KRH <i>in situ</i> gel	kKP	27.996	0.9390	0.9323	71.2228	1.9849	0.394
	MRT <i>in situ</i> gel	kKP	33.001	0.9495	0.9439	66.5959	2.0277	0.306
Hopfenberg F=100*[1-(1-kHB*t)^n]	ATV-PCL NPs	kHB	0.045	0.6863	0.6514	90.5575	0.2438	3.000
	CS/ATV-PCL NPs	kHB	0.027	0.3967	0.3297	94.9929	-0.6030	4.500
	KRH <i>in situ</i> gel	kHB	0.025	0.7252	0.6947	87.7864	0.4791	4.500
	MRT <i>in situ</i> gel	kHB	0.022	0.4275	0.3639	93.3070	-0.4006	4.500
Baker-Lonsdale 3/2*[1-(1-F/100)^(2/3)]-F/100=kBL*t	ATV-PCL NPs	kBL	0.017	0.9447	0.9447	69.4644	2.1614	-
	CS/ATV-PCL NPs	kBL	0.013	0.8233	0.8233	79.4846	0.8069	-
	KRH <i>in situ</i> gel	kBL	0.013	0.9629	0.9629	63.7520	2.6640	-
	MRT <i>in situ</i> gel	kBL	0.009	0.8305	0.8305	77.9204	0.9982	-
Peppas-Sahlin	ATV-PCL NPs	k1	43.282	0.9972	0.9965	40.7642	4.7705	0.450

F=k1*t^m+k2*t^(2*m)	CS/ATV-PCL NPs	k1	49.735	0.9914	0.9893	50.1839	3.4706	0.322
	KRH <i>in situ</i> gel	k1	35.231	0.9900	0.9875	53.3502	3.6096	0.450
	MRT <i>in situ</i> gel	k1	38.604	0.9967	0.9959	38.6571	4.5676	0.450
Weibull F=100*[1-Exp[-((t-Ti)^β)/α]]	ATV-PCL NPs	β	0.483	0.9974	0.9967	40.0227	4.8379	-
	CS/ATV-PCL NPs	β	0.355	0.9904	0.9880	51.4618	3.3544	-
	KRH <i>in situ</i> gel	β	0.517	0.9952	0.9939	45.3729	4.3349	-
	MRT <i>in situ</i> gel	β	0.401	0.9909	0.9887	49.6923	3.5644	-

*Best fit release kinetic models for ATV-loaded PCL NPs shown with colored; In all models, F is the fraction (%) of drug released in time t, k0: zero-order release constant, k1: first-order release constant, kH: Higuchi release constant, kKP: release constant incorporating structural and geometric characteristics of the drug-dosage form, n: is the diffusional exponent indicating the drug-release mechanism, m: diffusional exponent and similar exponent like "n", m use in Peppas-Sahlin model equation only, α: is the scale parameter which defines the time scale of the process; β: the shape parameter which characterizes the curve as either exponential (β=1; case 1), sigmoid, S-shaped, with upward curvature followed by a turning point (β > 1; case 2), or parabolic, with a higher initial slope and after that consistent with the exponential (β < 1; case 3), Ti: the location parameter which represents the lag time before the onset of the dissolution or release process and in most cases will be near zero. Values shown in grey in the table are selections made according to criteria.

Table 6. Calculation of the differences and similarities of the release profiles of the formulations with the difference (f1) and similarity (f2) factors

Formulations		Difference factor (f1)	Similarity factor (f2)
ATV-PCL NPs	CS/ATV-PCL NPs	7.03	64.59
KRH <i>in situ</i> gel	MRT <i>in situ</i> gel	6.51	69.41
ATV-PCL NPs	KRH <i>in situ</i> gel	13.01	54.27
CS/ATV-PCL NPs	MRT <i>in situ</i> gel	12.15	54.56

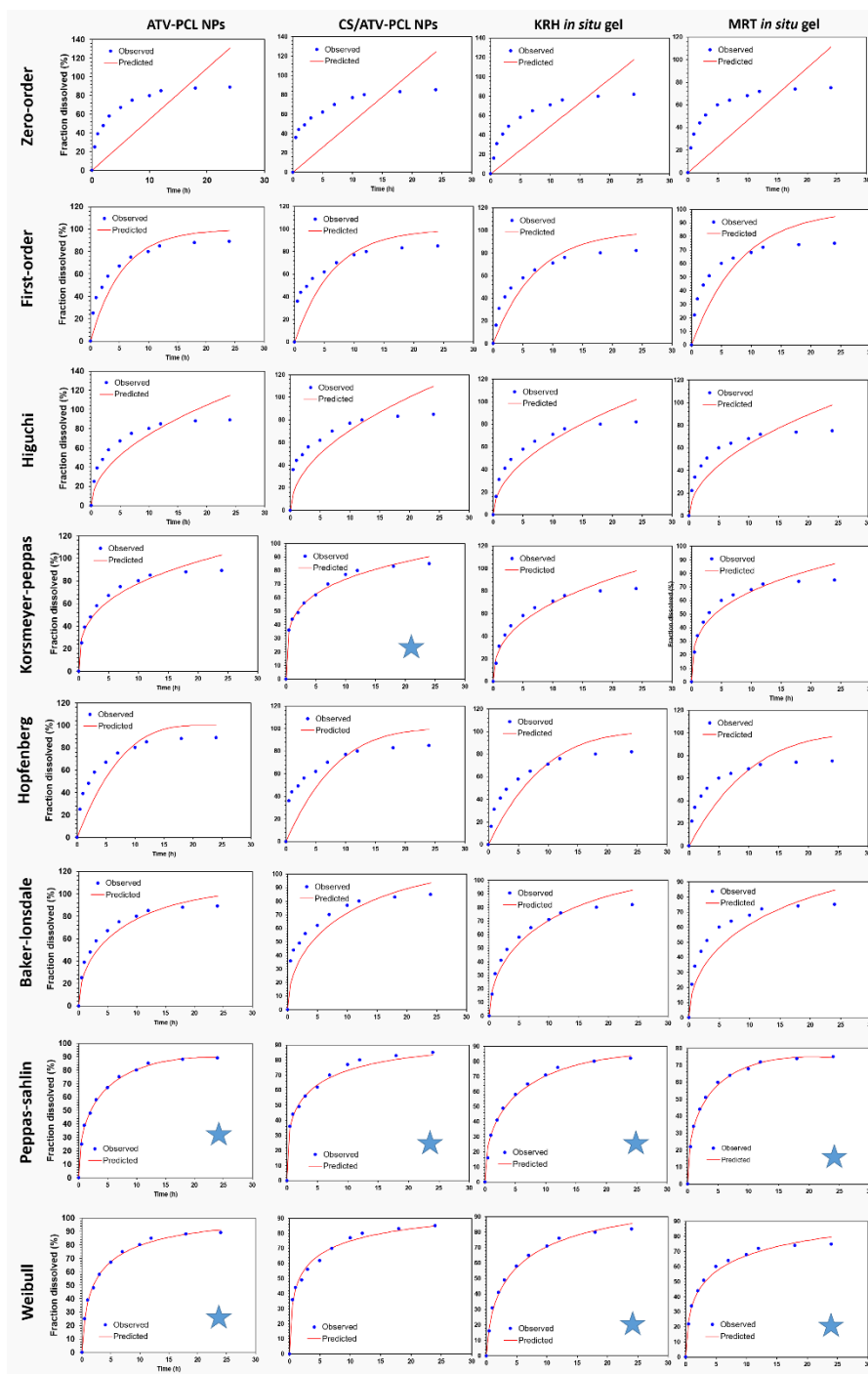


Figure 7. Mathematical model fitting of ATV release from PCL NPs for Zero-order, first-order, Higuchi, Korsmeyer-Peppas, Peppas-Sahlin, Weibull, Hopfenberg, and Baker-Lonsdale models.

3. CONCLUSION

In this study, we developed *in situ* gel formulation containing PCL-NPs loaded with ATV showing antioxidant and anti-inflammatory effects. In particular, the periodontal pocket cases which is suitable environment for bacterial growth, result in serious health problems owing to inflammation. The aim of this

study was to suppress inflammation in periodontal pockets. To this end, we developed *in situ* gel formulation loaded with ATV-PCL NPs. Results showed that size of NPs ranges from 176 nm to 329 nm. They exhibited 59% encapsulation efficiency and prolonged release. To prolong the release time and enhance the mucoadhesive properties, *in situ* gel system was developed and PCL-NPs were loaded to *in situ* gel formulation. The findings showed that *in situ* gel significantly increased the release time of ATV. According to results *in situ* gel systems designed for periodontal pockets can be effective in the future.

4. MATERIALS AND METHODS

Polycaprolactone (PCL) (Mw:14.000 and Mw:80.000), Atorvastatin, HPMC, PL 407, Acetone and dialysis cellulose tubing membrane (average flat width 25 mm, MWCO: 14,000 Da) were purchased from Sigma&Aldrich, USA. Chitosan (Protasan UP G-113; Mw:<200 kDa) was purchased from Novamatrix, Norway. All other chemicals used were of analytical grade and obtained from Sigma&Aldrich.

4.1. Preparation of blank and ATV-loaded PCL nanoparticles by nanoprecipitation

Blank and ATV-loaded PCL nanoparticles were prepared by nanoprecipitation method [58]. To prepare PCL NPs, phases were prepared as shown in Table 9. Organic phase was added to aqueous phase at a ratio of 1:2. Finally, supernatants were filtered through 0.45 µm pore size filter. Same process was carried out for blank formulations. Finally, each formulation was freeze-dried for other steps. To this end, first they were stored at -20C for 24 hours. Then NP formulations were put into freeze dryer so water in the formulations under low pressure is removed.

Table 7. Preparation protocol of PCL NPs

Step	Parameter	Values
1	<i>Organic phase</i>	
	PCL concentration	0.5% and 0.25 % w/v PCL
	Amount of ATV for drug loaded NPs	1% w/w of total PCL concentration
	Amount of Acetone	5 mL
2	<i>Aqueous Phase</i>	
	Pluronic F-68	75 mg
	Chitosan	0.025 %w/v
	Amount of ultra-pure water	10 mL
3	Mixing of phases	2 hours
4	Evaporation of the organic solvent	24 hours
5	Centrifugation of NPs	10 minutes
Step	Notes	
1	To prepare organic phase, two different amounts of PCL polymer, 25 mg and 12.5 mg, and ATV at the 1% of the polymer was firstly dissolved in 5 mL acetone. Solutions were stirred for 45 min.	

- 2 For the preparation of aqueous phase, 75 mg of Pluronic F-68 and 0,025% w/v chitosan were added to 10 mL ultra-pure water and stirred at 500 rpm.
- 3 Organic phase was added dropwise at the rate of 2mL/min under moderate magnetic stirrer at 800 rpm for 2 hours.
- 4 Organic solvent was evaporated at room temperature for 24 hours.
- 5 Dispersions were centrifuged at 3500 rpm for 5 min to precipitate unencapsulated drug and excess of polymer.

4.2. Characterization of Nanoparticles

4.2.1. Determination of particle size, PDI and surface charge

Determination of average particle diameter, zeta potential and polydispersity index for each PCL NPs were performed by dynamic light scattering (DLS) (Malvern Zetasizer Nano ZS series, UK)[58]. All measurements were performed at an angle of 173° for particle diameter and 12.8° for zeta potential. Measurements of the samples were conducted at room temperature (n=3). Particle size distribution was calculated as mean diameter (nm) ± standard deviation (SD) and PDI values were measured. Zeta potential (mV) was expressed as the average of three subsequent measurements ± SD.

4.2.2. Morphological analysis

The morphology of ATV-loaded PCL NPs was determined by using scanning electron microscopy (SEM) (Zeiss evo LS-10, Germany). The lyophilized PCL NPs were placed on a metal stub, then coated with 100 Å thick layer of gold and palladium and dried for 24 h in order to conduct the SEM imaging.

4.2.3. Determination of drug loading and entrapment efficiency

The lyophilized PCL NPs (3 mg) from each sample were dispersed in 300 µL dichloromethane (DCM) and vortexed for 10 min in order to break down the polymer structure. 3 mL of methanol was then added, and dichloromethane is evaporated by stirring at 500 rpm for 2 hours. Final dispersion was centrifuged 3000 rpm for 5 min. Encapsulated drug in the supernatant was assayed by the validated spectrophotometric method at 238 nm. Linearity, specificity, precision, repeatability, limit of detection (LOD), limit of quantification (LOQ) were determined as validation parameters. Drug Loading (DL) and Entrapment Efficiency (EE) were calculated using the following equations.

$$DL (\%) = (\text{Weight of ATV in the NPs} / \text{Total weight of NPs}) \times 100 \quad (1)$$

$$EE (\%) = (\text{Weight of ATV in NPs} / \text{Initial weight of ATV used}) \times 100 \quad (2)$$

4.2.4. *In vitro* ATV release from PCL nanoparticles

The *in vitro* cumulative release profile of ATV from PCL nanoparticles was determined by using dialysis membrane technique [59]. 2 mL of ATV-loaded NP formulation was placed into dialysis membrane (MWCO: 14,000 Da). The dialysis bag was immersed into 75 mL phosphate buffer saline (PBS) (pH 7.4) at 37°C. The system was stirred at 200 rpm. The samples were taken from the medium at predetermined time intervals (0.5, 1, 2, 4, 8, 16, 24, 36, 48, 72, 96h) and immediately replaced with PBS at the same volume to maintain sink condition. The cumulative percentage of total ATV was evaluated by validated spectroscopic method. The amount of released ATV in PBS was calculated with UV spectrophotometer at 246 nm. All measurements were repeated three times.

4.3. Preparation and Characterization of *in situ* Gel

4.3.1. Preparation of *in situ* gel

In situ gels were prepared by the cold method [60]. According to *in vitro* characterization studies of *in situ* gel formulations including pH, syringeability, determination of gelation time and temperature, one of the four formulations was selected to be used in release studies and determination of kinetic models. ATV-loaded NPs was incorporated to the chosen *in situ* gel formulation. When the literature regarding *in situ* gel formulations containing poloxamer was reviewed, it is reported that formulations containing more than 15% poloxamer show gelation behaviour at body temperature. In addition to that, formulations containing PL 407 at a concentration higher than 25% leads to gelation at room temperature [61]. Accordingly, to prepare *in situ* gel formulations, four different PL 407 ratios were determined as shown in Table 2. Each sample was kept at 2-8°C until they were used. Table 2 displays the final *in situ* gel formulations.

Table 8. Protocol of *in situ* gel preparation.

Code	Polymer	Ratio
1	PL 407	15% w/w, 18% w/w, 21% w/w, and 24% w/w
2	HPMC	1% w/w

Step	Notes
1	15% w/w, 18% w/w, 21% w/w, and 24% w/w PL 407 were dissolved in distilled water with gentle stirring for TB1, TB2, TB3, and TB4, respectively, until a homogenous dispersion was obtained. The obtained dispersions were stored in refrigerator at 2-8°C overnight in order to ensure complete dissolution.
2	The HPMC solution was added to the PL 407 solution the following day, agitated for an hour, and then overnight stored at 2-8°C.

4.3.2. pH

The pH of the formulations was measured using a pH meter (Fungilab viscometer (USA)). Three measurements in total were taken and the average measurements was computed (n=3).

4.3.3. Syringeability

In order to assess the syringeability of the *in situ* gel formulations, the method as described by Maheshwari et al. was followed [62]. Since high temperatures may lead to gelation of formulations, syringeability tests must be carried out with samples stored at +4°C. 1 mL of the gel formulation kept at +4°C was put into a 20 gauge needle syringe prior to be tested for flowability at standard handling pressure. The formulation, which were rapidly passed from the syringe was called passing.

4.3.4. Gelation temperature

Each polymer solution (10 mL) was stirred with a magnetic stirrer in a water bath. The heated polymer solutions were swirled at 100 rpm at 1°C/min (Thermomac-TM19). The temperature at which the magnetic bar cannot move was marked as the gelling temperature. Each was subjected to three measurements.

4.3.5. Determination of gelation time

In order to determine the gelation time of *in situ* gel formulations, the tube inversion technique was used (Asasutjarit et al., 2011). A test tube containing 2 mL of *in situ* gel kept at 4°C was immediately placed in the water bath set at the gelation temperature (35°C). By turning the test tube upside-down at regular

intervals, the *in situ* gel formation was observed. When there was no flow in the reversed test tube the gelation time was recorded.

4.3.6. Viscosity and Rheological Behaviour

Viscosity measurements of *in situ* gels was carried out using a rotational viscometer (Fungilab, USA) with a R5 spindle running at 10 rpm. The viscosities of all *in situ* gels were measured at both 25°C and 37°C and at 10 rpm (Table 3). Three measurements were taken for each sample [63].

At the gelation temperature viscosity was measured at spindle rotation of 1, 5, 10, 25, and 50 rpm in triplicate. Viscosity values versus various angular velocities were plotted to give flow curves. At the gelation temperature, the viscosity of *in situ* gels was measured. At various angular velocities, viscosities were measured, and flow curves were calculated. The test was carried out three times.

4.3.7. In Vitro Release from *in situ* gel

In vitro drug release of ATV from the *in situ* gel formulations was determined by dialysis bag diffusion method [64]. 1 mL of each gel formulation was added into dialysis membrane, hermetically sealed, and then embedded into 25 mL of an isotonic phosphate buffer (pH 7.4) at 37°C. *In vitro* release studies were conducted under sink conditions. At predetermined times (0, 0.5, 1, 2, 4, 7, 10, 12, and 14 days), samples were withdrawn, and replaced with equivalent quantities of the fresh buffer. ATV concentrations were determined using a UV-vis spectrophotometer. The total amount of ATV released from each formulation over time was recorded. The measurements were performed in triplicate.

4.3.8. Release Kinetic

A mathematical modelling study was used to portray the experimentally observed ATV release kinetics. Drug release results were computed using DDSolver program which shortens calculation time and avoids computational mistakes. Data were fitted to zero-order, first-order, Higuchi, Hopfenberg, Baker-Lonsdale, Peppas-Sahlin, and Weibull models [47]. Results were computed using the DDSolver to determine the four crucial parameters; coefficient of determination (R²), coefficient of determination adjusted (R²_{adjusted}), Akaike Information Criterion (AIC), and Model Selection Criterion (MSC). The maximum R², R²_{adjusted}, and MSC values and the minimum AIC values indicated best fit model. Moreover, release differences of formulations were calculated by DDSolver in terms of “difference (f1)” and “similarity (f2)” factor. If f1 is lower than 15 and f2 is between 50-100, release profile of formulations is similar to each other [65].

Acknowledgements: This research was not financially supported by any organization. This research did not receive any specific grant from funding agencies in the public, commercial, or not-for-profit sectors.

Author contributions: Concept: S.Ü., O.D.; Design: S.Ü., O.D.; Control: S.Ü., O.D., H.K.P.; Sources: S.Ü., O.D., H.K.P.; Materials: S.Ü., O.D., H.K.P.; Data Collection and/or processing: S.Ü., O.D., H.K.P.; Analysis and/or interpretation: S.Ü., O.D., H.K.P.; Literature review: S.Ü., O.D., H.K.P.; Manuscript writing: S.Ü., O.D., H.K.P., YA; Critical review: S.Ü., O.D., H.K.P., YA; Other: S.Ü.

Conflict of interest statement: The authors declare that there is no real, potential, or perceived conflict of interest for this article.

REFERENCES

- [1] Melcher, A. H. On the repair potential of periodontal tissues. *Journal of Periodontology*. 1976; 47(5): 256-260. <https://doi.org/10.1902/jop.1976.47.5.256>
- [2] Pragati, S., Ashok, S., & Kuldeep, S. Recent advances in periodontal drug delivery systems. *International Journal of Drug Delivery*. 2009; 1(1). <http://doi.org/10.5138/ijdd.2009.0975.0215.01001>
- [3] Tatakis, D. N., Kumar, P. S. Etiology and pathogenesis of periodontal diseases. *Dent Clin North Am*. 2005; 49(3) 491-516. <https://doi.org/10.1016/j.cden.2005.03.001>

- [4] Kim, W. J., Soh, Y., & Heo, S. M. Recent Advances of Therapeutic Targets for the Treatment of Periodontal Disease. *Biomol Ther (Seoul)*. 2021; 29(3): 263-267. <https://doi.org/10.4062/biomolther.2021.001>
- [5] Jain, M. K., & Ridker, P. M. Anti-inflammatory effects of statins: clinical evidence and basic mechanisms. *Nat Rev Drug Discov*. 2005; 4(12): 977-987. <https://doi.org/10.1038/nrd1901>
- [6] Barsante, M. M., Roffe, E., Yokoro, C. M., Tafuri, W. L., Souza, D. G., Pinho, V., Castro, M.S.A., Teixeira, M. M. Anti-inflammatory and analgesic effects of atorvastatin in a rat model of adjuvant-induced arthritis. *Eur J Pharmacol*. 2005; 516(3): 282-289. <https://doi.org/10.1016/j.ejphar.2005.05.005>
- [7] Shao, Q., Shen, L. H., Hu, L. H., Pu, J., Jing, Q., & He, B. Atorvastatin suppresses inflammatory response induced by oxLDL through inhibition of ERK phosphorylation, I κ B α degradation, and COX-2 expression in murine macrophages. *Journal of Cellular Biochemistry*. 2012; 113(2): 611-618. <https://doi.org/10.1002/jcb.23388>
- [8] Zamvil, S. S., & Steinman, L. Cholesterol-lowering statins possess anti-inflammatory activity that might be useful for treatment of MS. *Neurology*. 2002; 59: 970-971
- [9] Armitage, J. The safety of statins in clinical practice. *Lancet*. 2007; 370(9601): 1781-1790. [https://doi.org/10.1016/S0140-6736\(07\)60716-8](https://doi.org/10.1016/S0140-6736(07)60716-8)
- [10] Sierra, S., Ramos, M. C., Molina, P., Esteo, C., Vazquez, J. A., & Burgos, J. S. Statins as Neuroprotectants: A Comparative In Vitro Study of Lipophilicity, Blood-Brain-Barrier Penetration, Lowering of Brain Cholesterol, and Decrease of Neuron Cell Death. *Journal of Alzheimers Disease*. 2011; 23(2): 307-318. <https://doi.org/10.3233/Jad-2010-101179>
- [11] Begines, B., Ortiz, T., Perez-Aranda, M., Martinez, G., Merinero, M., Arguelles-Arias, F., & Alcudia, A. Polymeric Nanoparticles for Drug Delivery: Recent Developments and Future Prospects. *Nanomaterials (Basel)*. 2020; 10(7): 1403. <https://doi.org/10.3390/nano10071403>
- [12] Khalid, M., & El-Sawy, H. S. Polymeric nanoparticles: Promising platform for drug delivery. *International Journal of Pharmaceutics*. 2017; 528(1-2): 675-691. <https://doi.org/10.1016/j.ijpharm.2017.06.052>
- [13] Gou, M., Wei, X., Men, K., Wang, B., Luo, F., Zhao, X., Wei, Y., Qian, Z. PCL/PEG copolymeric nanoparticles: potential nanoplatfoms for anticancer agent delivery. *Curr Drug Targets*. 2011; 12(8): 1131-1150. <https://doi.org/10.2174/138945011795906642>
- [14] Mondrinos, M. J., Dembzyński, R., Lu, L., Byrapogu, V. K., Wootton, D. M., Lelkes, P. I., & Zhou, J. Porogen-based solid freeform fabrication of polycaprolactone-calcium phosphate scaffolds for tissue engineering. *Biomaterials*. 2006; 27(25): 4399-4408. <https://doi.org/10.1016/j.biomaterials.2006.03.049>
- [15] Wei, X., Gong, C., Gou, M., Fu, S., Guo, Q., Shi, S., Luo, F., Guo, G., Qiu, L., Qian, Z. Biodegradable poly (ϵ -caprolactone)-poly (ethylene glycol) copolymers as drug delivery system. *International Journal of Pharmaceutics*. 2009; 381(1): 1-18. <https://doi.org/10.1016/j.ijpharm.2009.07.033>
- [16] Yamamoto, M., Ikada, Y., & Tabata, Y. Controlled release of growth factors based on biodegradation of gelatin hydrogel. *J Biomater Sci Polym Ed*. 2001; 12(1): 77-88. <https://doi.org/10.1163/156856201744461>
- [17] Tangpasuthadol, V., Pongchaisirikul, N., & Hoven, V. P. Surface modification of chitosan films. Effects of hydrophobicity on protein adsorption. *Carbohydr Res*. 2003; 338(9): 937-942. [https://doi.org/10.1016/s0008-6215\(03\)00038-7](https://doi.org/10.1016/s0008-6215(03)00038-7)
- [18] Wilsonjr, O., & Hull, J. Surface modification of nanophased hydroxyapatite with chitosan. *Materials. Sci. Eng. C*. 2008; 28: 434-437. <https://doi.org/10.1016/j.msec.2007.04.005>
- [19] Badran, M. M., Mady, M. M., Ghannam, M. M., & Shakeel, F. Preparation and characterization of polymeric nanoparticles surface modified with chitosan for target treatment of colorectal cancer. *Int J Biol Macromol*. 2017; 95: 643-649. <https://doi.org/10.1016/j.ijbiomac.2016.11.098>
- [20] Nasra, M. M., Khiri, H. M., Hazzah, H. A., & Abdallah, O. Y. Formulation, in-vitro characterization and clinical evaluation of curcumin in-situ gel for treatment of periodontitis. *Drug Delivery*. 2017; 24(1): 133-142. <https://doi.org/10.1080/10717544.2016.1233591>
- [21] Beg, S., Dhiman, S., Sharma, T., Jain, A., Sharma, R. K., Jain, A., & Singh, B. Stimuli Responsive In Situ Gelling Systems Loaded with PLGA Nanoparticles of Moxifloxacin Hydrochloride for Effective Treatment of Periodontitis. *AAPS Pharmscitech*. 2020; 21(3): 76. <https://doi.org/10.1208/s12249-019-1613-7>

- [22] Polat H.K. In Situ Gels Triggered by Temperature for Ocular Delivery of Dexamethasone and Dexamethasone/SBE- β -CD Complex. *J.Res.Pharm.* 2022; 26(4): 873-883. <http://dx.doi.org/10.29228/jrp.186>
- [23] Badri, W., Miladi, K., Nazari, Q. A., Fessi, H., & Elaissari, A. Effect of process and formulation parameters on polycaprolactone nanoparticles prepared by solvent displacement. *Colloids and Surfaces a-Physicochemical and Engineering Aspects.* 2017; 516: 238-244. <https://doi.org/10.1016/j.colsurfa.2016.12.029>
- [24] Tavares, M. R., de Menezes, L. R., Dutra, J. C., Cabral, L. M., & Tavares, M. I. B. Surface-coated polycaprolactone nanoparticles with pharmaceutical application: Structural and molecular mobility evaluation by TD-NMR. *Polymer Testing* 2017; 60: 39-48. <https://doi.org/10.1016/j.polymertesting.2017.01.032>
- [25] Varan, C., & Bilensoy, E. Cationic PEGylated polycaprolactone nanoparticles carrying post-operation docetaxel for glioma treatment. *Beilstein J Nanotechnol.* 2017; 8(1): 1446-1456. <https://doi.org/10.3762/bjnano.8.144>
- [26] Gaumet, M., Vargas, A., Gurny, R., & Delie, F. Nanoparticles for drug delivery: the need for precision in reporting particle size parameters. *Eur J Pharm Biopharm.* 2008; 69(1): 1-9. <https://doi.org/10.1016/j.ejpb.2007.08.001>
- [27] Longmire, M., Choyke, P. L., & Kobayashi, H. Clearance properties of nano-sized particles and molecules as imaging agents: considerations and caveats. *Nanomedicine.* 2008; 3(5): 703-717. <https://doi.org/10.2217/17435889.3.5.703>
- [28] Sukhanova, A., Bozrova, S., Sokolov, P., Berestovoy, M., Karaulov, A., & Nabiev, I. Dependence of Nanoparticle Toxicity on Their Physical and Chemical Properties. *Nanoscale Research Letters.* 2018; 13(1), 1-21. <https://doi.org/ARTN.4410.1186/s11671-018-2457-x>
- [29] Chorny, M., Fishbein, I., Danenberg, H. D., & Golomb, G. Lipophilic drug loaded nanospheres prepared by nanoprecipitation: effect of formulation variables on size, drug recovery and release kinetics. *J Control Release.* 2002; 83(3): 389-400. [https://doi.org/10.1016/s0168-3659\(02\)00211-0](https://doi.org/10.1016/s0168-3659(02)00211-0)
- [30] Miladi, K., Sfar, S., Fessi, H., & Elaissari, A. Encapsulation of alendronate sodium by nanoprecipitation and double emulsion: From preparation to *in vitro* studies. *Industrial Crops and Products.* 2015; 72: 24-33. <https://doi.org/10.1016/j.indcrop.2015.01.079>
- [31] Colmenares Roldán, G. J., Agudelo Gomez, L. M., Carlos Cornelio, J. A., Rodriguez, L. F., Pinal, R., & Hoyos Palacio, L. M. Production of polycaprolactone nanoparticles with low polydispersity index in a tubular recirculating system by using a multifactorial design of experiments. *Journal of Nanoparticle Research.* 2018; 20(3): 1-12. <https://doi.org/10.1007/s11051-018-4168-8>
- [32] Rasmussen, M. K., Pedersen, J. N., & Marie, R. Size and surface charge characterization of nanoparticles with a salt gradient. *Nat Commun.* 2020; 11(1): 2337. <https://doi.org/10.1038/s41467-020-15889-3>
- [33] Jo, D. H., Kim, J. H., Lee, T. G., & Kim, J. H. Size, surface charge, and shape determine therapeutic effects of nanoparticles on brain and retinal diseases. *Nanomedicine.* 2015; 11(7): 1603-1611. <https://doi.org/10.1016/j.nano.2015.04.015>
- [34] Yang, S. C., Ge, H. X., Hu, Y., Jiang, X. Q., & Yang, C. Z. Formation of positively charged poly(butyl cyanoacrylate) nanoparticles stabilized with chitosan. *Colloid and Polymer Science.* 2000; 278(4): 285-292. <https://doi.org/DOI.10.1007/s003960050516>
- [35] Budhian, A., Siegel, S. J., & Winey, K. I. Haloperidol-loaded PLGA nanoparticles: systematic study of particle size and drug content. *Int J Pharm.* 2007; 336(2): 367-375. <https://doi.org/10.1016/j.ijpharm.2006.11.061>
- [36] Mikusova, V., & Mikus, P. Advances in Chitosan-Based Nanoparticles for Drug Delivery. *Int J Mol Sci.* 2021; 22(17): 9652. <https://doi.org/10.3390/ijms22179652>
- [37] Varan, G., Benito, J. M., Mellet, C. O., & Bilensoy, E. Development of polycationic amphiphilic cyclodextrin nanoparticles for anticancer drug delivery. *Beilstein J Nanotechnol.* 2017; 8(1): 1457-1468. <https://doi.org/10.3762/bjnano.8.145>
- [38] Nagarwal, R. C., Kumar, R., & Pandit, J. K. Chitosan coated sodium alginate-chitosan nanoparticles loaded with 5-FU for ocular delivery: *in vitro* characterization and *in vivo* study in rabbit eye. *Eur J Pharm Sci.* 2012; 47(4): 678-685. <https://doi.org/10.1016/j.ejps.2012.08.008>
- [39] Permana, A. D., Utami, R. N., Layadi, P., Himawan, A., Juniarti, N., Anjani, Q. K., Utomo, E., Mardikasari, S.A., Arjuna, A., Donnelly, R. F. Thermosensitive and mucoadhesive *in situ* ocular gel for effective local delivery and

- antifungal activity of itraconazole nanocrystal in the treatment of fungal keratitis. *Int J Pharm.* 2021; 602: 120623. <https://doi.org/10.1016/j.ijpharm.2021.120623>
- [40] Reed, K. L., Malamed, S. F., & Fonner, A. M. Local anesthesia part 2: technical considerations. *Anesth Prog.* 2012; 59(3): 127-136. <https://doi.org/10.2344/0003-3006-59.3.127>
- [41] Du, L., Tong, L., Jin, Y., Jia, J., Liu, Y., Su, C., Yu, S., Li, X. A multifunctional *in situ*-forming hydrogel for wound healing. *Wound Repair Regen.* 2012; 20(6): 904-910. <https://doi.org/10.1111/j.1524-475X.2012.00848.x>
- [42] Balasingam, R., Khan, A., & Thinakaran, R. Formulation of *in Situ* Gelling System for Ophthalmic Delivery of Erythromycin. *Int J Students' Res Technol Manag.* 2017; 5(3): 01-08.
- [43] Wanka, G., Hoffmann, H., & Ulbricht, W. Phase-Diagrams and Aggregation Behavior of Poly(Oxyethylene)-Poly(Oxypropylene)-Poly(Oxyethylene) Triblock Copolymers in Aqueous-Solutions. *Macromolecules.* 1994; 27(15): 4145-4159. <https://doi.org/DOI.10.1021/ma00093a016>
- [44] El-Enin, A. A., & El-Feky, G. Formulation and evaluation of *in-situ* gelling tenoxicam liquid suppositories. *J. of Life Medicine.* 2013; (1): 2
- [45] Abd Elhady, S. S., Mortada, N. D., Awad, G. A., & Zaki, N. M. Development of *in situ* gelling and muco adhesive mebeverine hydrochloride solution for rectal administration. *Saudi Pharmaceutical Journal.* 2003; 11.
- [46] Morsi, N., Ghorab, D., Refai, H., & Teba, H. Ketorolac tromethamine loaded nanodispersion incorporated into thermosensitive *in situ* gel for prolonged ocular delivery. *International Journal of Pharmaceutics.* 2016; 506(1-2): 57-67. <https://doi.org/10.1016/j.ijpharm.2016.04.021>
- [47] Zhang, Y., Huo, M., Zhou, J., Zou, A., Li, W., Yao, C., & Xie, S. DDSolver: an add-in program for modeling and comparison of drug dissolution profiles. *AAPS J.* 2010; 12(3): 263-271. <https://doi.org/10.1208/s12248-010-9185-1>
- [48] Patil, A. Preparation, characterization and toxicity evaluation of a novel sustained release delivery system for a hydrogen sulfide donor-GYY 4137. 2016; Creighton University.
- [49] Fathalla, Z. M. A., Vangala, A., Longman, M., Khaled, K. A., Hussein, A. K., El-Garhy, O. H., & Alany, R. G. Poloxamer-based thermoresponsive ketorolac tromethamine *in situ* gel preparations: Design, characterisation, toxicity and transcorneal permeation studies. *European Journal of Pharmaceutics and Biopharmaceutics.* 2017; 114: 119-134. <https://doi.org/10.1016/j.ejpb.2017.01.008>
- [50] Laddha, U. D., & Kshirsagar, S. J. Formulation of nanoparticles loaded *in situ* gel for treatment of dry eye disease: *In vitro*, *ex vivo* and *in vivo* evidences. *Journal of Drug Delivery Science and Technology.* 2021; 61: 102112. <https://doi.org/ARTN.102112>
- [51] Chu, K., Chen, L., Xu, W., Li, H., Zhang, Y., Xie, W., & Zheng, J. Preparation of a paeonol-containing temperature-sensitive *in situ* gel and its preliminary efficacy on allergic rhinitis. *Int J Mol Sci.* 2013; 14(3): 6499-6515. <https://doi.org/10.3390/ijms14036499>
- [52] Munot, N. M., Kishore, G., & Mithila, K. Development and evaluation of biodegradable microspheres embedded in *in situ* gel for controlled delivery of hydrophilic drug for treating oral infections: *In vitro* and *in vivo* studies. *Asian Journal of Pharmaceutics (AJP).* 2014; 8(3). <https://doi.org/10.22377/ajp.v8i3.358>
- [53] Yang, H., Li, J., Patel, S. K., Palmer, K. E., Devlin, B., & Rohan, L. C. Design of Poly(lactic-co-glycolic Acid) (PLGA) Nanoparticles for Vaginal Co-Delivery of Griffithsin and Dapivirine and Their Synergistic Effect for HIV Prophylaxis. *Pharmaceutics.* 2019; 11(4): 184. <https://doi.org/10.3390/pharmaceutics11040184>
- [54] Ozturk, A. A., Yenilmez, E., & Ozarda, M. G. Clarithromycin-Loaded Poly (Lactic-co-glycolic Acid) (PLGA) Nanoparticles for Oral Administration: Effect of Polymer Molecular Weight and Surface Modification with Chitosan on Formulation, Nanoparticle Characterization and Antibacterial Effects. *Polymers (Basel).* 2019; 11(10): 1632. <https://doi.org/10.3390/polym11101632>
- [55] Rehman, M., Ihsan, A., Madni, A., Bajwa, S. Z., Shi, D., Webster, T. J., & Khan, W. S. Solid lipid nanoparticles for thermoresponsive targeting: evidence from spectrophotometry, electrochemical, and cytotoxicity studies. *Int J Nanomedicine.* 2007; 12: 8325-8336. <https://doi.org/10.2147/IJN.S147506>
- [56] Papadopoulou, V., Kosmidis, K., Vlachou, M., & Macheras, P. On the use of the Weibull function for the discernment of drug release mechanisms. *Int J Pharm.* 2006; 309(1-2): 44-50. <https://doi.org/10.1016/j.ijpharm.2005.10.044>

- [57] Ainurofiq, A., & Choiri, S. Drug Release Mechanism of Slightly Soluble Drug from Nanocomposite Matrix Formulated with Zeolite/Hydrotalcite as Drug Carrier. *Tropical Journal of Pharmaceutical Research*. 2015; 14(7): 1129-1135. <https://doi.org/10.4314/tjpr.v14i7.2>
- [58] Unal, S., Aktas, Y., Benito, J. M., & Bilensoy, E. Cyclodextrin nanoparticle bound oral camptothecin for colorectal cancer: Formulation development and optimization. *Int J Pharm*. 2020; 584: 119468. <https://doi.org/10.1016/j.ijpharm.2020.119468>
- [59] Bilensoy, E., Gürkaynak, O., Doğan, A. L., & Hıncal, A. A. Safety and efficacy of amphiphilic β -cyclodextrin nanoparticles for paclitaxel delivery. *International Journal of Pharmaceutics*. 2008; 47(1-2): 163-170. <https://doi.org/10.1016/j.ijpharm.2007.06.051>
- [60] Polat H.K. Design of Metformin HCl and Moxifloxacin HCl Loaded Thermosensitive In Situ Gel. *J.Res.Pharm*. 2022; 26(5): 1230-1241. <http://dx.doi.org/10.29228/jrp.215>
- [61] Almeida, H., Amaral, M. H., Lobao, P., & Sousa Lobo, J. M. Applications of poloxamers in ophthalmic pharmaceutical formulations: an overview. *Expert Opin Drug Deliv*. 2013; 10(9): 1223-1237. <https://doi.org/10.1517/17425247.2013.796360>
- [62] Maheshwari, M., Miglani, G., Mali, A., Paradkar, A., Yamamura, S., & Kadam, S. Development of tetracycline-serratiopeptidase-containing periodontal gel: formulation and preliminary clinical study. *AAPS Pharmscitech*. 2006; 7(3): 76. <https://doi.org/10.1208/pt070376>
- [63] Wanka, G., Hoffmann, H., & Ulbricht, W. (1995). *Macromolecules* 1994, 27, 4145.[ACS Full Text ACS Full Text], Google Scholar There is no corresponding record for this reference.(b) Alexandridis, P.; Hatton, TA. *Colloids Surf. A*, 96, 1.
- [64] Polat, H. K., Kurt, N., Aytakin, E., Akdağ Çaylı, Y., Bozdağ Pehlivan, S., & Çalış, S. Design of Besifloxacin HCl-Loaded Nanostructured Lipid Carriers: In Vitro and Ex Vivo Evaluation. *J Ocul Pharmacol Ther*. 2022; 38(6): 412-423. <https://doi.org/10.1089/jop.2022.0008>
- [65] Puthli, S., & Vavia, P. R. Stability studies of microparticulate system with piroxicam as model drug. *AAPS Pharmscitech*. 2009; 10(3): 872-880. <https://doi.org/10.1208/s12249-009-9280-8>

This is an open access article which is publicly available on our journal's website under Institutional Repository at <http://dspace.marmara.edu.tr>.